

Image Fusion Transformer

Vibashan VS, *Student Member, IEEE*, Jeya Maria Jose Valanarasu, *Student Member, IEEE*, Poojan Oza, *Student Member, IEEE*, and Vishal M. Patel, *Senior Member, IEEE*

Abstract—In image fusion, images obtained from different sensors are fused to generate a single image with enhanced information. In recent years, state-of-the-art methods have adopted Convolution Neural Networks (CNNs) to encode meaningful features for image fusion. Specifically, CNN-based methods perform image fusion by fusing local features. However, they do not consider long-range dependencies that are present in the image. Transformer-based models are designed to overcome this by modeling the long-range dependencies with the help of self-attention mechanism. This motivates us to propose a novel Image Fusion Transformer (IFT) where we develop a transformer-based multi-scale fusion strategy that attends to both local and long-range information (or global context). The proposed method follows a two-stage training approach. In the first stage, we train an auto-encoder to extract deep features at multiple scales. In the second stage, multi-scale features are fused using a Spatio-Transformer (ST) fusion strategy. The ST fusion blocks are comprised of a CNN and a transformer branch which capture local and long-range features, respectively. Extensive experiments on multiple benchmark datasets show that the proposed method performs better than many competitive fusion algorithms. Furthermore, we show the effectiveness of the proposed ST fusion strategy with an ablation analysis. The source code is available at: <https://github.com/Vibashan/Image-Fusion-Transformer>.

Index Terms—Image fusion, Transformer, CNN.

I. INTRODUCTION

IMAGE fusion has proved to be critical in many real world applications, e.g., military [1], computer vision [2], remote sensing [3], and medical imaging [4]. It refers to combining different images of the same scene to integrate complementary information and generate a single fused image. For example, the images captured using a visible sensor are rich in fine details like color, contrast, and texture. However, visible sensors fail to distinguish between objects and background under poor lighting conditions. The images obtained using thermal sensors capture salient features that distinguish objects from the background during daytime and nighttime. However, thermal sensors lack texture and color space information about the object. This is because visible sensors work in 300-530 μm wavelength while thermal sensors work in 8-14 μm wavelength [5]. It would be very useful to have a single image that contains complementary information from visible and thermal sensors. Image fusion specifically tackles this by fusing the complementary attributes from different sources to generate a detailed scene representation [6].

Traditional methods for image fusion include sparse representation (SR) based methods [8], [9]; multi-scale transformation based methods [10], [11]; saliency-based methods

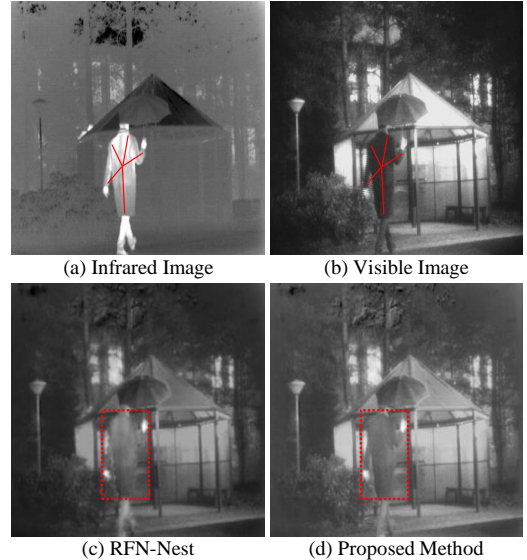


Fig. 1. (a) Infrared source image, (b) Visible source image. Image fusion results using (c) RFN-Nest [7] and proposed method (d) Image Fusion Transformer (IFT). The red line highlights all pixels that belong to the foreground (human). The red box highlights the foreground object fusion by RFN-Nest and IFT. In RFN-Nest, we can observe a gradual decrease of intensity from the top part to the bottom part of the human. This can be explained due to the lack of long-range feature learning capability of CNN-based RFN-Nest. However, IFT does well in encoding these long-range dependencies resulting in the same pixel intensity of the human. Hence, we observe a stark difference in the boundary between foreground and background objects when compared to RFN-Nest.

[12], [13] and low-rank representation (LRR) based methods [14], [15]. Even though these methods achieve competitive performance, there exists several shortcomings: 1) They have a poor generalization ability as they rely on handcrafted feature extraction, 2) Dictionary learning in SR and LRR is time-consuming [7], and 3) Different sets of source images require different fusion strategies.

Recent image fusion works have explored CNN-based fusion techniques [16], [7], [17], which outperform traditional ones by overcoming the aforementioned shortcomings. Though existing CNN-based fusion techniques improve generalization ability by learning local features, they fail to extract long-range dependencies in the images. This results in the loss of some essential global context that might be useful for an exemplary fused image. Therefore we argue that integrating local features with long-range dependencies can add global contextual information, which in turn helps to improve fusing performance further. With this motivation, we propose an Image Fusion Transformer (IFT) with a novel Spatio-Transformer (ST) fusion strategy that effectively learns both local features and long-range information at multiple scales to fuse the complementary information from given images (see Fig. 1). The main contributions of this work can

Vibashan VS, Jeya Maria Jose Valanarasu, Poojan Oza, Vishal M. Patel are with Department of Electrical and Computer Engineering in Johns Hopkins University, Baltimore, MD 21218, USA. (e-mail: {vvishnu2, jvalana1, poza2, vpatel36}@jhu.edu).

be summarized as follows:

- We propose a novel fusion method, called Image Fusion Transformer (IFT), that utilizes both local information and models long-range dependencies to overcome the lack of global contextual understanding that exists in recent image fusion works.
- The proposed method utilizes a novel Spatio-Transformer (ST) fusion strategy, where a spatial CNN branch and a transformer branch are employed to utilize both local and global features to fuse the given images better.
- The proposed method is evaluated on multiple fusion benchmark datasets, where we achieve competitive results compared to the existing fusion methods.

II. RELATED WORKS

A. Image fusion

Traditional image fusion methods employed discrete cosine transform (DCT) [18], sparse representation (SR) [19], [8], principal component analysis (PCA) [20], etc. to extract useful features. However, these feature extraction methods lack generalizability. Moreover, images captured from different sources require different fusion strategies. As a result, traditional fusion strategies are designed in a source-specific manner.

To overcome these issues with the traditional methods, deep learning-based approaches were introduced for image fusion. Li [16] proposed a technique where at first, the visible and thermal images are decomposed. Later, they perform fusion using the decomposed images by average feature fusion and deep learning-based feature fusion. Another work proposed by Li [21] uses a fully convolution-based model to fuse the visible and thermal images. Here, features from source images are extracted using a DenseNet encoder and fused using a CNN-based fusion layer. A CNN-based decoder is then used to get the fused image. Li [7] further extended their previous work [21] to an end-to-end fusion strategy for multi-scale deep features minimizing the proposed detail and feature loss. Xu [17] proposed a unified unsupervised end-to-end framework that tackles the fusion problem by integrating it with continual learning. However, all of these methods focus on learning spatial local features between source images and do not consider the long-range dependencies present within the source images. In this work we explore extracting long-range features in addition to the local features to enhance the fusion quality further.

B. Transformers

Transformer model architecture was first proposed by Vaswani [22] and has been proven to be extremely important in Natural Language Processing (NLP) literature over the years [23], [24], [25]. The success of transformer-based models can be attributed to their ability to capture better long-range information compared to recurrent neural networks and CNNs. Motivated by their success, Dosovitskiy proposed a Vision Transformer (ViT) [26] for image classification. This has sparked a significant interest in developing transformer-based methods for vision problems like object detection [27], [28]

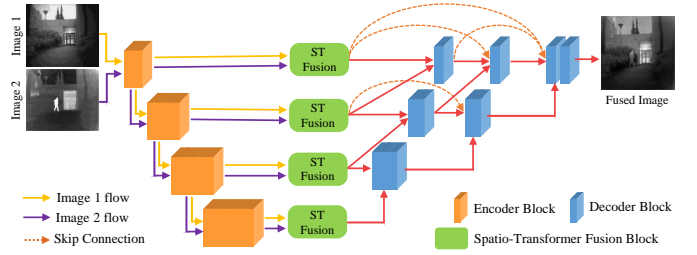


Fig. 2. Overview of the proposed Image Fusion Transformer (IFT) network. Image 1 and Image 2 are passed through the encoder to obtain multi-scale deep features. These extracted deep features are fused using the Spatio-Transformer (ST) fusion block. Finally, the decoder reconstructs the multi-scale fused features to output a fused image.

and segmentation [29], [30]. Hence, in this work, we also exploit a transformer-based architecture to obtain improved image fusion performance by enabling the model to encode long-range dependencies from the images.

III. PROPOSED METHOD

A. Image Fusion Transformer (IFT)

The proposed Image Fusion Transformer (IFT) is a fusion network which takes in any number of input source images and generates an enhanced fused image. IFT consists of three parts: encoder network, Spatio-Transformer (ST) fusion network and a nested decoder network as illustrated in Fig. 2. The encoder network consists of four encoder blocks, where each encoder block contains a convolution layer with kernel size 3×3 followed by ReLU and max-pooling operation. For a given source input, we extract deep features at multiple-scales from each convolution block of the encoder network. These extracted features from both images are then fused at multiple scales using the ST fusion network. The ST fusion network consists of a spatial branch and a transformer branch. The spatial branch consists of conv layers and a bottleneck layer to capture local features. The transformer branch consists of an axial attention-based transformer block to capture long-range dependencies (or global context). Finally, we obtain the fused image by training the nested decoder network with the fused features as an input. The decoder network is based on the RFN-Nest [7] architecture.

B. Self-attention and axial-attention

Self-attention is an attention mechanism that relates different tokens of a single sequence in order to compute a representation of the same sequence. Let $x \in \mathbb{R}^{C_{in} \times H \times W}$ and $y \in \mathbb{R}^{C_{out} \times H \times W}$ be the input and output features where C_{in} and C_{out} are the number of input and output channels, respectively and H and W correspond to height and width, respectively. The output y is computed as follows:

$$y_{ij} = \sum_{h=1}^H \sum_{w=1}^W \text{softmax}(q_{ij}^T k_{hw}) v_{hw}, \quad (1)$$

where q_{ij} , k_{ij} and v_{ij} are query, key and value at any arbitrary location $i \in \{1, \dots, H\}$ and $j \in \{1, \dots, W\}$ and are computed as $q = W_Q x$, $k = W_K x$ and $v = W_V x$, respectively. From Eq. 1, we can infer that self-attention computes long-range affinities

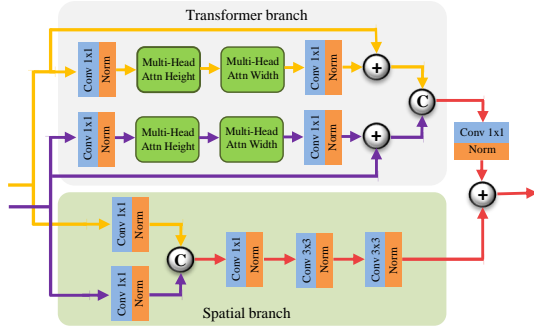


Fig. 3. The feed-forward path for Spatio-Transformer (ST) fusion mechanism. The encoded feature maps from Image 1 and Image 2 are fed to the spatial branch and the transformer branch. The spatial branch extracts fine local features while the transformer branch extracts long-range features.

throughout the entire feature map unlike CNN. However, this self-attention mechanism is computationally expensive due to their quadratic complexity.

Hence, we employ the axial attention mechanism [31] which is computationally more efficient. Specifically, in axial attention, self-attention is first performed over the feature map height axis and then over the width axis thus reducing computational complexity. Moreover, Wang [32], proposed a learnable positional embedding to axial attention query, key and value to make the affinities sensitive to the positional information. These positional embeddings are parameters that are learnt jointly during training. Therefore, for a given input x , the self-attention along the height axis can be computed as:

$$y_{ij} = \sum_{h=1}^H \text{softmax}(q_{ij}^T k_{ih} + q_{ij}^T r_{ih}^q + k_{ij}^T r_{ih}^k)(v_{ih} + v_{ih}) \quad (2)$$

where $r^q, r^k, r^v \in \mathbb{R}^{H \times H}$ are the positional embedding for height axis. For axial attention, we compute Eq. 2 along both height and width axis, which provides a computation efficient self-attention model.

C. Spatio-Transformer (ST) fusion strategy

The proposed ST fusion block consists of two branches, namely, spatial and transformer branch. In the spatial branch, we use a conv block and a bottleneck layer to capture local features. In the transformer branch, we use axial attention to learn global-contextual features by modeling long-range dependencies through the self-attention mechanism. We add these two features to obtain a fused feature map containing enhanced local and global-context information. Moreover, we applied our ST fusion strategy at multiple scales and then forwarded it to the decoder network to obtain the final fused image. ST fusion block is illustrated in Fig. 3.

D. Loss function

The proposed method is trained to preserve fine structural details and retain the salient foreground and background details. The overall training objective to train IFT, denoted as L_{fuse} , can be given as:

$$L_{fuse} = L_{feat} + \alpha L_{det}, \quad (3)$$

where L_{det} is the structural similarity loss, which is computed as follows

$$L_{det} = 1 - SSIM(O, I) \quad (4)$$

where O and I are the fused and input source image, respectively. Also, $SSIM(\cdot)$ measures structural similarity [33]. If $SSIM(O, I)$ tends to 1, then the fused image retains most of the structural details from the source images and vice versa. The feature similarity loss L_{feat} is calculated as follows

$$L_{feat} = \sum_{m=1}^M w_1 \|\Phi_f^m - (w_{I1}\Phi_{I1}^m + w_{I2}\Phi_{I2}^m)\|_F^2, \quad (5)$$

where M is the number scales at which deep features are extracted; $f, I1, I2$ denote fused image, input source 1 image and input source 2 image, respectively. Also, w_1, w_{I1}, w_{I2} are trade off parameters to balance the loss magnitude. Φ_f^m is the fused feature map while Φ_{I1} and Φ_{I2} correspond to the encoded feature maps of the input source 1 and input source 2 images, respectively. This loss constrains the fused deep features to preserve salient structures, thus enhancing the fused feature space to learn more salient features and preserve fine details. Here, α is a hyperparameter.

IV. EXPERIMENTS AND RESULTS

A. Implementation details

For visible and infrared fusion, we train our model on 80000 pairs of visible and infrared images in the KAIST dataset. We test on 21 pairs of visible and infrared images in the TNO Human Factors dataset during testing. Further, we follow RFN-Nest experimental setup by resizing the images to 256×256 and setting hyperparameters $w_{I1}, w_{I2}, w_1, \alpha$ equal to 6, 3, 100, 700. For all experiments, we set the learning rate, epoch, and batch size equal to 10^{-4} , 4 and 2, respectively.

For the experiment with MRI and PET images, the network is trained on 9981 cropped patches with image pairs obtained from the Harvard MRI and PET datasets. The trained model is evaluated on 20 pairs of MRI and PET images sampled from the Harvard MRI and PET image fusion dataset. During training, we resize the images to 84×84 and convert the PET images to IHS scale to fuse the I channel with an MRI image. For all experiments, we set the learning rate, epoch, and batch size equal to 10^{-4} , 4 and 2, respectively. Our network is based on PyTorch and implemented on NVIDIA TITAN Xp GPU.

B. Infrared and visible image fusion

From Table I, we can observe that the proposed method outperforms the existing methods in En and MI metrics. Our method can capture both local and long-range dependencies generating sharper content and preserve most of the visual information compared to other methods. Further, our method produces competitive performance in SCD and MS-SSIM metrics than other methods solely focusing on local image fusion. Qualitative fusion results are illustrated in the top row of Fig. 4. The red box highlights the human and the yellow box highlights the reconstruction of fine features. In the red box, we can observe that capturing long-range dependencies results

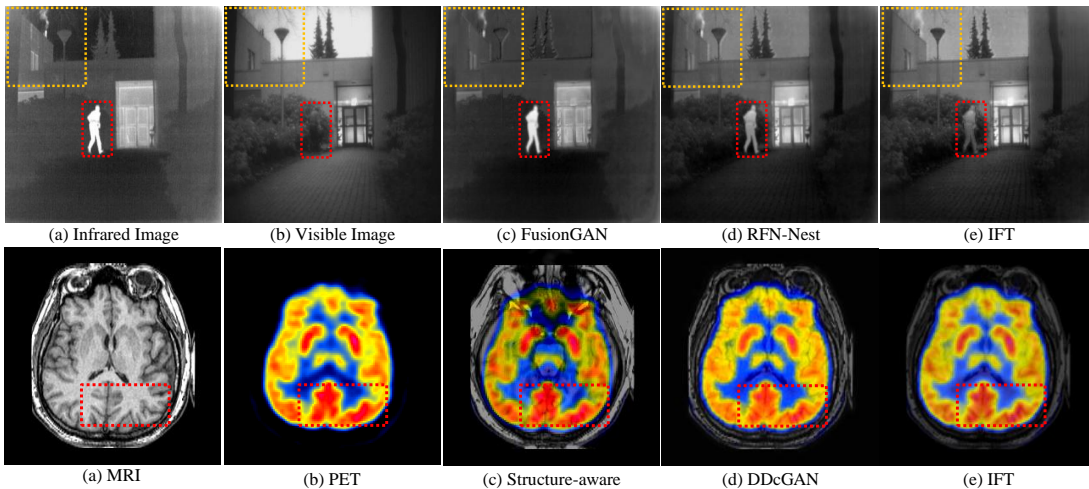


Fig. 4. Qualitative comparison: (1) *Top* : Infrared/Visible; (2) *Bottom* : MRI/PET. Other fusion methods lack do not focus on modeling long-range dependencies while our proposed method encodes both local and global-context, resulting in a better fusion.

in assigning the same intensity all over the human for IFT compared to other CNN-based methods. In addition, we can observe in the yellow box that our model can reconstruct fine details as it captures both long-range and local information.

TABLE I
QUANTITATIVE RESULTS ON 21 PAIRS OF INFRARED AND VISIBLE IMAGES. EN: ENTROPY, SCD: SUM OF THE CORRELATIONS OF DIFFERENCES, MI: MUTUAL INFORMATION, MS-SSIM: MULTI-SCALE STRUCTURAL SIMILARITY.

Methods	En [34]	SCD [35]	MI [36]	MS-SSIM [33]
DCHWT [37]	6.5677	1.6099	13.1355	0.8432
ConvSR [38]	6.2586	1.6482	12.5173	0.9028
VggML [16]	6.1826	1.6352	12.3652	0.8747
DenseFuse [21]	6.6715	1.8350	13.3431	0.9289
IFCNN [39]	6.5954	1.7137	13.1909	0.9052
NestFuse [40]	6.9197	1.7335	13.8394	0.8624
FusionGan [41]	6.3628	1.4568	12.7257	0.7318
U2Fusion [17]	6.7570	1.7983	13.5141	0.9253
RFN-Nest [7]	6.8413	1.8367	13.6826	0.9145
IFT	6.9862	1.7818	13.9725	0.8606

C. MRI and PET image fusion

From Table II, we can infer that our method outperforms all the existing methods in Entropy and CC metrics by preserving local and long-range information. In SD and MG metrics, it produces competitive performance compared to the existing techniques. Qualitative fusion results are illustrated in the bottom row of Fig. 4 and the red box highlights the intensity variation of PET colors in the fused image. From Fig. 4 we can observe that Structure-aware method [42] lacks color intensity variations in the fused image; whereas, DDcGAN and IFT exhibit better intensity variations and brighter colors. Moreover, IFT color variation is more similar to PET than DDcGAN, thanks to IFT’s ability to encode long-range dependencies. This can be also observed from the high performance in Correlation Coefficient (CC) metric from Table II.

D. Ablation Study

An ablation study is conducted on the ST Fusion branch and the results are reported in Table III. Spatial-based image fusion performs fusion using only local features, whereas

TABLE II
QUANTITATIVE RESULTS FOR 20 PAIRS OF MRI AND PET IMAGE FUSION. EN: ENTROPY, SD: STANDARD DEVIATION, CC: CORRELATION COEFFICIENT, MG: MEAN GRADIENT.

Methods	En [34]	SD [43]	CC [44]	MG [44]
DCHWT [37]	5.7507	0.3337	0.8510	0.0448
DDCTPCA [45]	5.2298	0.3351	0.9044	0.0257
Structure-Aware [42]	5.1144	0.3426	0.8390	0.0454
FusionGAN [41]	5.1841	0.1741	0.8547	0.0198
RCGAN [46]	5.6549	0.2894	0.9000	0.0303
DDcGAN [44]	5.9787	0.3519	0.9012	0.0471
IFT	6.4328	0.3298	0.9463	0.0444

transformer-based image fusion performs fusion operation utilizing long-range dependencies. However, it is crucial to capture both local and long-range features for understanding overall representation, which results in better image fusion. From Table III, it is evident that our proposed ST fusion network outperforms only spatial or transformer-based image fusion in all metrics by capturing both local and long-range dependencies. Hence, this supports our argument that image fusion is improved by integrating long-range dependencies with local features.

TABLE III
ABLATION STUDY ON THE ST FUSION NETWORK FOR MRI AND PET IMAGE FUSION.

Methods	En [34]	SD [43]	CC [44]	MG [44]
Spatial	5.9813	0.2961	0.9311	0.0382
Transformer	6.1459	0.3183	0.9392	0.0418
IFT (Spatial+Transformer)	6.4328	0.3298	0.9463	0.0444

V. CONCLUSION

In this work, we proposed an Image Fusion Transformer (IFT) network where we developed a novel Spatio-Transformer (ST) fusion strategy that attends to both local and long-range dependencies. In the ST fusion strategy, a CNN branch and a transformer branch are introduced to fuse local and global features. The proposed method is evaluated on multiple fusion benchmark datasets where we achieve better results compared to the existing fusion methods. Moreover, we perform an ablation study to show the effectiveness of extracting local and long-range information while doing fusion.

REFERENCES

- [1] J. Ma, Y. Ma, and C. Li, "Infrared and visible image fusion methods and applications: A survey," *Information Fusion*, vol. 45, pp. 153–178, 2019.
- [2] C. Lopez-Molina, J. Montero, H. Bustince, and B. De Baets, "Self-adapting weighted operators for multiscale gradient fusion," *Information Fusion*, vol. 44, pp. 136–146, 2018.
- [3] M. Eslami and A. Mohammadzadeh, "Developing a spectral-based strategy for urban object detection from airborne hyperspectral tir and visible data," *IEEE Journal of Selected Topics in Applied Earth Observations and Remote Sensing*, vol. 9, no. 5, pp. 1808–1816, 2015.
- [4] S. Li, X. Kang, L. Fang, J. Hu, and H. Yin, "Pixel-level image fusion: A survey of the state of the art," *information Fusion*, vol. 33, pp. 100–112, 2017.
- [5] J. Tian, Y. Leng, Z. Zhao, Y. Xia, Y. Sang, P. Hao, J. Zhan, M. Li, and H. Liu, "Carbon quantum dots/hydrogenated tio2 nanobelt heterostructures and their broad spectrum photocatalytic properties under uv, visible, and near-infrared irradiation," *Nano Energy*, vol. 11, pp. 419–427, 2015.
- [6] X. Jin, Q. Jiang, S. Yao, D. Zhou, R. Nie, J. Hai, and K. He, "A survey of infrared and visual image fusion methods," *Infrared Physics & Technology*, vol. 85, pp. 478–501, 2017.
- [7] H. Li, X.-J. Wu, and J. Kittler, "Rfn-nest: An end-to-end residual fusion network for infrared and visible images," *Information Fusion*, vol. 73, pp. 72–86, 2021.
- [8] Y. Bin, Y. Chao, and H. Guoyu, "Efficient image fusion with approximate sparse representation," *International Journal of Wavelets, Multiresolution and Information Processing*, vol. 14, no. 04, p. 1650024, 2016.
- [9] Q. Zhang, Y. Fu, H. Li, and J. Zou, "Dictionary learning method for joint sparse representation-based image fusion," *Optical Engineering*, vol. 52, no. 5, p. 057006, 2013.
- [10] H.-M. Hu, J. Wu, B. Li, Q. Guo, and J. Zheng, "An adaptive fusion algorithm for visible and infrared videos based on entropy and the cumulative distribution of gray levels," *IEEE Transactions on Multimedia*, vol. 19, no. 12, pp. 2706–2719, 2017.
- [11] K. He, D. Zhou, X. Zhang, R. Nie, Q. Wang, and X. Jin, "Infrared and visible image fusion based on target extraction in the nonsubsampling contourlet transform domain," *Journal of Applied Remote Sensing*, vol. 11, no. 1, p. 015011, 2017.
- [12] J. Ma, Z. Zhou, B. Wang, and H. Zong, "Infrared and visible image fusion based on visual saliency map and weighted least square optimization," *Infrared Physics & Technology*, vol. 82, pp. 8–17, 2017.
- [13] C. Liu, Y. Qi, and W. Ding, "Infrared and visible image fusion method based on saliency detection in sparse domain," *Infrared Physics & Technology*, vol. 83, pp. 94–102, 2017.
- [14] G. Liu, Z. Lin, Y. Yu *et al.*, "Robust subspace segmentation by low-rank representation," in *icml*, vol. 1. Citeseer, 2010, p. 8.
- [15] G. Liu, Z. Lin, S. Yan, J. Sun, Y. Yu, and Y. Ma, "Robust recovery of subspace structures by low-rank representation," *IEEE transactions on pattern analysis and machine intelligence*, vol. 35, no. 1, pp. 171–184, 2012.
- [16] H. Li, X.-J. Wu, and J. Kittler, "Infrared and visible image fusion using a deep learning framework," in *2018 24th international conference on pattern recognition (ICPR)*. IEEE, 2018, pp. 2705–2710.
- [17] H. Xu, J. Ma, J. Jiang, X. Guo, and H. Ling, "U2fusion: A unified unsupervised image fusion network," *IEEE Transactions on Pattern Analysis and Machine Intelligence*, 2020.
- [18] L. Cao, L. Jin, H. Tao, G. Li, Z. Zhuang, and Y. Zhang, "Multi-focus image fusion based on spatial frequency in discrete cosine transform domain," *IEEE signal processing letters*, vol. 22, no. 2, pp. 220–224, 2014.
- [19] Q. Zhang, Y. Liu, R. S. Blum, J. Han, and D. Tao, "Sparse representation based multi-sensor image fusion for multi-focus and multi-modality images: A review," *Information Fusion*, vol. 40, pp. 57–75, 2018.
- [20] L. I. Kuncheva and W. J. Faithfull, "Pca feature extraction for change detection in multidimensional unlabeled data," *IEEE transactions on neural networks and learning systems*, vol. 25, no. 1, pp. 69–80, 2013.
- [21] H. Li and X.-J. Wu, "Densefuse: A fusion approach to infrared and visible images," *IEEE Transactions on Image Processing*, vol. 28, no. 5, pp. 2614–2623, 2018.
- [22] A. Vaswani, N. Shazeer, N. Parmar, J. Uszkoreit, L. Jones, A. N. Gomez, L. Kaiser, and I. Polosukhin, "Attention is all you need," *arXiv preprint arXiv:1706.03762*, 2017.
- [23] Z. Dai, Z. Yang, Y. Yang, J. Carbonell, Q. V. Le, and R. Salakhutdinov, "Transformer-xl: Attentive language models beyond a fixed-length context," *arXiv preprint arXiv:1901.02860*, 2019.
- [24] J. Devlin, M.-W. Chang, K. Lee, and K. Toutanova, "Bert: Pre-training of deep bidirectional transformers for language understanding," *arXiv preprint arXiv:1810.04805*, 2018.
- [25] N. Kitaev, L. Kaiser, and A. Levskaya, "Reformer: The efficient transformer," *arXiv preprint arXiv:2001.04451*, 2020.
- [26] A. Dosovitskiy, L. Beyer, A. Kolesnikov, D. Weissenborn, X. Zhai, T. Unterthiner, M. Dehghani, M. Minderer, G. Heigold, S. Gelly *et al.*, "An image is worth 16x16 words: Transformers for image recognition at scale," *arXiv preprint arXiv:2010.11929*, 2020.
- [27] X. Zhu, W. Su, L. Lu, B. Li, X. Wang, and J. Dai, "Deformable detr: Deformable transformers for end-to-end object detection," *arXiv preprint arXiv:2010.04159*, 2020.
- [28] N. Carion, F. Massa, G. Synnaeve, N. Usunier, A. Kirillov, and S. Zagoruyko, "End-to-end object detection with transformers," in *European Conference on Computer Vision*. Springer, 2020, pp. 213–229.
- [29] H. Wang, Y. Zhu, H. Adam, A. Yuille, and L.-C. Chen, "Max-deeplab: End-to-end panoptic segmentation with mask transformers," in *Proceedings of the IEEE/CVF Conference on Computer Vision and Pattern Recognition*, 2021, pp. 5463–5474.
- [30] J. M. J. Valanarasu, P. Oza, I. Hacihaliloglu, and V. M. Patel, "Medical transformer: Gated axial-attention for medical image segmentation," *arXiv preprint arXiv:2102.10662*, 2021.
- [31] J. Ho, N. Kalchbrenner, D. Weissenborn, and T. Salimans, "Axial attention in multidimensional transformers," *arXiv preprint arXiv:1912.12180*, 2019.
- [32] H. Wang, Y. Zhu, B. Green, H. Adam, A. Yuille, and L.-C. Chen, "Axial-deeplab: Stand-alone axial-attention for panoptic segmentation," in *European Conference on Computer Vision*. Springer, 2020, pp. 108–126.
- [33] K. Ma, K. Zeng, and Z. Wang, "Perceptual quality assessment for multi-exposure image fusion," *IEEE Transactions on Image Processing*, vol. 24, no. 11, pp. 3345–3356, 2015.
- [34] J. W. Roberts, J. A. Van Aardt, and F. B. Ahmed, "Assessment of image fusion procedures using entropy, image quality, and multispectral classification," *Journal of Applied Remote Sensing*, vol. 2, no. 1, p. 023522, 2008.
- [35] V. Aslantas and E. Bendes, "A new image quality metric for image fusion: the sum of the correlations of differences," *Aeu-international Journal of electronics and communications*, vol. 69, no. 12, pp. 1890–1896, 2015.
- [36] G. Qu, D. Zhang, and P. Yan, "Information measure for performance of image fusion," *Electronics letters*, vol. 38, no. 7, pp. 313–315, 2002.
- [37] B. S. Kumar, "Multifocus and multispectral image fusion based on pixel significance using discrete cosine harmonic wavelet transform," *Signal, Image and Video Processing*, vol. 7, no. 6, pp. 1125–1143, 2013.
- [38] Y. Liu, X. Chen, R. K. Ward, and Z. J. Wang, "Image fusion with convolutional sparse representation," *IEEE signal processing letters*, vol. 23, no. 12, pp. 1882–1886, 2016.
- [39] Y. Zhang, Y. Liu, P. Sun, H. Yan, X. Zhao, and L. Zhang, "Ifcnn: A general image fusion framework based on convolutional neural network," *Information Fusion*, vol. 54, pp. 99–118, 2020.
- [40] H. Li, X.-J. Wu, and T. Durrani, "Nestfuse: An infrared and visible image fusion architecture based on nest connection and spatial/channel attention models," *IEEE Transactions on Instrumentation and Measurement*, vol. 69, no. 12, pp. 9645–9656, 2020.
- [41] J. Ma, W. Yu, P. Liang, C. Li, and J. Jiang, "Fusiongan: A generative adversarial network for infrared and visible image fusion," *Information Fusion*, vol. 48, pp. 11–26, 2019.
- [42] W. Li, Y. Xie, H. Zhou, Y. Han, and K. Zhan, "Structure-aware image fusion," *Optik*, vol. 172, pp. 1–11, 2018.
- [43] Y.-J. Rao, "In-fibre bragg grating sensors," *Measurement science and technology*, vol. 8, no. 4, p. 355, 1997.
- [44] J. Ma, H. Xu, J. Jiang, X. Mei, and X.-P. Zhang, "Ddcgan: A dual-discriminator conditional generative adversarial network for multi-resolution image fusion," *IEEE Transactions on Image Processing*, vol. 29, pp. 4980–4995, 2020.
- [45] V. Naidu, "Hybrid ddct-pca based multi sensor image fusion," *Journal of Optics*, vol. 43, no. 1, pp. 48–61, 2014.
- [46] Q. Li, L. Lu, Z. Li, W. Wu, Z. Liu, G. Jeon, and X. Yang, "Coupled gan with relativistic discriminators for infrared and visible images fusion," *IEEE Sensors Journal*, 2019.